Materials Science and Engineering C 51 (2015) 256–262

Contents lists available at ScienceDirect

Materials Science and Engineering C

journal homepage: www.elsevier.com/locate/msec

Tautomerizable β-ketonitrile copolymers for bone tissue engineering: Studies of biocompatibility and cytotoxicity

M. Laura Lastra [a], M. Silvina Molinuevo [a,*], Juan M. Giussi [b,c], Patricia E. Allegretti [c], Iwona Blaszczyk-Lezak [d], Carmen Mijangos [d], M. Susana Cortizo [b,*]

[a] Laboratorio de Investigaciones en Osteopatías y Metabolismo Mineral (LIOMM), Facultad de Ciencias Exactas, UNLP (1900), 47 y 115, 1900 La Plata, Argentina
[b] Instituto de Investigaciones Fisicoquímicas Teóricas y Aplicadas (INIFTA), CCT-La Plata, CC16 suc. 4, 1900 La Plata, Argentina
[c] Laboratorio de Estudio de Compuestos Orgánicos (LADECOR), Facultad de Ciencias Exactas, UNLP, 47 y 115, 1900 La Plata, Argentina
[d] Instituto de Ciencia y Tecnología de Polímeros, CSIC, Juan de la Cierva 3, 28006 Madrid, Spain

ARTICLE INFO

Article history:
Received 2 December 2014
Received in revised form 2 February 2015
Accepted 9 March 2015
Available online 11 March 2015

Keywords:
Tautomeric copolymer
Bone tissue engineering
Biocompatibility
Cytotoxicity assays

ABSTRACT

β-Ketonitrile tautomeric copolymers have demonstrated tunable hydrophilicity/hydrophobicity properties according to surrounding environment, and mechanical properties similar to those of human bone tissue. Both characteristic properties make them promising candidates as biomaterials for bone tissue engineering. Based on this knowledge we have designed two scaffolds based on β-ketonitrile tautomeric copolymers which differ in chemical composition and surface morphology. Two of them were nanostructured, using an anodized aluminum oxide (AAO) template, and the other two obtained by solvent casting methodology. They were used to evaluate the effect of the composition and their structural modifications on the biocompatibility, cytotoxicity and degradation properties. Our results showed that the nanostructured scaffolds exhibited higher degradation rate by macrophages than casted scaffolds (6 and 2.5% of degradation for nanostructured and casted scaffolds, respectively), a degradation rate compatible with bone regeneration times. We also demonstrated that the β-ketonitrile tautomeric based scaffolds supported osteoblastic cell proliferation and differentiation without cytotoxic effects, suggesting that these biomaterials could be useful in the bone tissue engineering field.

1. Introduction

Polymeric materials based on tautomeric monomers have been designed to be used in many applications such as colloidal stabilization of hybrid nanomaterial, stimuli-responsive for biomedical uses or in order to enhance the thermo-mechanical properties [1–3]. The main advantage of this kind of polymers is the possibility to regulate the composition of both tautomeric forms (keto-enol) to obtain polymeric materials with changeable polarity as a function of the surrounding environment. This behavior has been previously demonstrated in a systematic study conducted by the polymerization of a β-ketonitrile monomer under different solvent conditions [4,5]. Thereby, the presence of tautomeric groups is especially important in these macromolecules to discriminate against specific substrates according to the environment in which they exist. A property that could make them interesting for biomedical applications. Many approaches to functionalize the scaffold surface or nanoparticles for drug delivery have been undertaken in order to introduce useful surface characteristics to provide the desired microenvironment for such goal [6,7]. For example, scaffolds are very important for good cell adhesion, proliferation and differentiation. On the other hand, a biomaterial suitable for bone tissue engineering should present mechanical properties similar to those of bone tissue in order to support the tensions of the skeleton during the regeneration time. We have previously demonstrated that these tautomeric copolymers presented appropriated thermal and mechanical properties to be used as a bone substitute [8]. In this sense, the ultimate tensile stress increments in the increase of the tautomeric monomer mole fraction of the copolymer, and the elastic modulus and the tensile strength of the copolymers reached values intermediate between trabecular and cortical bone.

In order to design adequate scaffolds for bone tissue engineering, several factors have to be taken into account including chemical composition, topographic characteristics, biocompatibility, cytotoxicity and mechanical properties [9,10]. One of the more relevant characteristic is the topography of the biomaterials, which may influence not only cell adhesion but also cell proliferation and differentiation. Cell adhesion to biomaterial surface is an important prerequisite for the successful integration of implants in vivo, as well as for cell colonization of scaffolds proposed for tissue engineering applications. In fact, some authors found that scaffolds with an ordered surface improve cellular biocompatibility, increasing cell development and differentiation and wound healing while decreasing inflammatory properties [9,11,12].

* Corresponding authors.
E-mail addresses: silvinamolinuevo@yahoo.com.ar (M.S. Molinuevo), gcortizo@infta.unlp.edu.ar (M.S. Cortizo).

http://dx.doi.org/10.1016/j.msec.2015.03.008
0928-4931/

In order to obtain scaffolds with nanofiber topography, different methodologies have been used such as electro-spraying and electro-spinning for polymer solution and melt-spinning for solid state polymer, and so on [13–15]. In the last years a new methodology based on patterning of alumina templates had been proposed in order to obtain one-dimensional ordered nanostructures. The advantage of this nanostructuration method is the possibility of preparing surface supported nanofibers which exhibited high or moderate aspect ratio and it can be applied to different polymeric materials [16–18]. This technique was successfully applied to obtain biodegradable extracellular matrices consisting of mechanically stable arrays of aligned poly(lactide) nanorods [19]. Fibroblasts growing on these nanorods formed dense tissue layers, with an excellent adhesion to the substrate and exhibited a highly elongated morphology similar to those occurring in natural tissue [19].

In the present study we analyzed the effect of the biomaterial composition and topography of a tautomerizable β-ketonitrile copolymer for bone tissue engineering. Two β-ketonitrile copolymers which differ in chemical composition and surface morphology were evaluated for biocompatibility, cytotoxicity and degradation properties.

2. Materials and methods

2.1. Materials

Styrene (98%, PASA S.A.) was freed from an inhibitor by washing with aqueous NaOH solution (10% wt) and then with water until neutrality, dried over anhydrous sodium sulfate and distilled under reduced pressure before use. The initiator, 2,2′-Azobis(isobutyronitrile) (AIBN, 98%, Merck) was purified by recrystallization from methanol before use. 2-Methyl-3-oxo-5-phenyl-4-pentenonitrile (MOP) was synthesized as previously reported [4]. Methanol (99.9%, Aldrich), chloroform (RPE, Carlo Erba), hydrochloric acid (37%, Merck), and $CuCl_2$ (97%, Aldrich) were used as received without further purification.

2.2. Polymer synthesis and characterization

Two tautomerizablestyrene-co-2-methyl-3-oxo-5-phenyl-4-pentenonitrile copo-lymers (St-co-MOP), of different MOP monomer mole fractions in the copolymer (F_{MOP}), were synthesized by mass radical polymerization and characterized following a procedure described elsewhere [4]. Briefly, different amounts of both co-monomers (total weight 10 mL) were introduced into a reaction tube with a preweighed amount of initiator (35 mM). The mixtures were degassed by three freeze–pump–thaw cycles in a vacuum line system, then sealed and immersed into a thermostat at 60 °C at different times in the absence of light. After the reaction, the polymer was isolated with methanol and purified by three steps of dissolutions in chloroform and precipitation in methanol. Finally, it was centrifuged and dried under vacuum.

The ^1H NMR spectra of the samples were recorded with a Bruker Spectrometer; 300 MHz. Chloroform-d_1 was used as solvent for the polymer. The polymer sample concentration was 6.0% of weight and the measurements were carried out at 40 °C.

The average molecular weight (M_w, M_n) and the molecular weight distribution (M_w/M_n) were determined by SEC in a LKB-2249 instrument at 25 °C. A series of four μ-Styragel columns (10^5, 10^4, 10^3, 100 Å pore size) were used with chloroform as eluent. The polymer concentration was 4–5 mg/mL, and the flow rate was 0.5 mL/min. The polymer was analyzed using double detection as previously reported. Mass chromatograms of the polymers were detected by a Shimadzu (SPD-10A) UV/VIS detector at 254 nm (for the phenyl group), while the carbonyl group was detected by infrared absorption at 5.75 μm with a Miram 1A spectrophotometer detector [20]. Polystyrene standards supplied by Polymer Laboratories and Polysciences were used for calibration.

2.3. Casting, nanostructuration and surface characterization of the scaffold

In the first case, the copolymer was casted as a film, (SC), prepared from a chloroform solution (5 wt.%) and was poured onto teflon dishes (19.6 cm^2). The solvent was allowed to evaporate at room temperature, and then the resulting films were dried under vacuum until constant weight. The films were washed with ethanol 70° and sterilized by UV exposition for 30 min. SEC confirmed that no degradation of the material had occurred during this treatment [21].

The nanostructured scaffolds, NS, were prepared by infiltration of copolymer via the melt precursor film wetting method into the anodized aluminum oxide (AAO) template of 270 nm and 15 μm of length (Fig. 1), as previously described [8,17]. Briefly, the solid copolymers were placed on the AAO surfaces and introduced in an oven, at a temperature about 100 °C higher than the copolymer glass transition temperature (T_g), under nitrogen atmosphere. After the infiltration process, the excess of copolymer was removed from the surface of AAO template with the aid of a razor.

In order to remove the AAO template and obtain the supported free nanofibers, previously, a coating of polymethyl methacrylate has been place over the template, then, templates were treated, in the first place with an aqueous solution of $CuCl_2$ and HCl and after that with 5 wt.% of phosphoric acid [8].

The scaffolds were designed as SC17 and SN17 for scaffolds obtained from St-co-MOP copolymer of 17% of MOP composition, and as SC62 and SN62, for the scaffolds corresponding to the copolymer of 62% of MOP composition.

The surface of both types of the scaffolds, SC and SN, with or without cells was coated with gold and their morphology was examined using scanning electron microscopy (SEM, Phillips505 Holland) and the images were analyzed by Soft Imaging System ADDAII.

Water contact angle (WCA) measurements were carried out using deionized water at room temperature, as previously published [22].

2.4. Swelling assay

The maximum swelling and water absorption capacity of the membranes (from SC or SN) were determined as follows [23]. The membranes were weighed (w_0) and then immersed in the phosphate-buffered saline (PBS, pH 7.4) at 37 °C. Then of 24 h, the samples were removed, and after wiping the surface with paper, were weighed in the wet state (w). The water content of the membrane was obtained as the difference between w, the weight of the water saturated sample and w_0, the weight

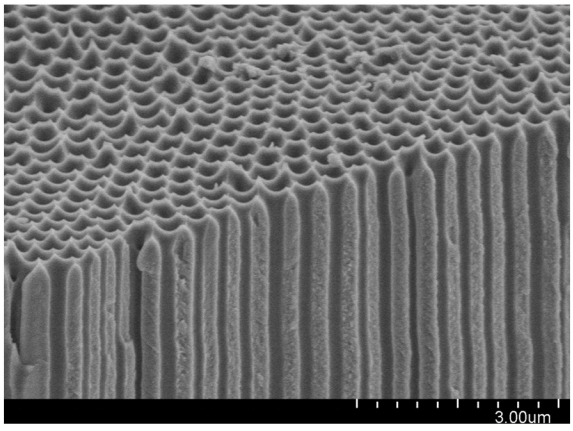

Fig. 1. Scanning electron microscopy (SEM) of AAO template.

of the initial dried sample. The percentage of swelling of the membrane is defined as:

$$\%S_w = \frac{100(w - w_0)}{w_0}. \quad (1)$$

2.5. Cell cultures and incubations

MC3T3E1 mouse calvaria-derived cells were grown in DMEM containing 10% FBS, 100 U/mL penicillin and 100 μg/mL streptomycin at 37 °C in a 5% CO_2 atmosphere. Cells were seeded on 75 cm^2 flasks and sub-cultured using trypsin-EDTA. In MC3T3E1 osteoblast-like cells, previous studies have demonstrated that expression of osteoblastic markers begins after culturing the cells with medium supplemented by 5 mM beta-glycerol-phosphate (βGP) and 25 μg/mL ascorbic acid [14,24]. Under these culture conditions, alkaline phosphatase activity begins to be expressed after 1 week and reaches a maximum after 2 weeks, while mineralization is achieved after extending the culture to 3 weeks. However, the cells only undergo active replication during the first 5 days of incubation. For adhesion and proliferation experiments and differentiation experiments, cells on polymeric matrix-coated dishes were incubated in 10% FBS medium during the periods of time indicated in the legend of figures. For collagen production and mineralization experiments with MC3T3E1 osteoblast cells were cultured for 2 weeks in an osteogenic media (DMEM/FBS supplemented with β-glycerol-phosphate and ascorbic acid) changing the medium every 2 days.

RAW264.7 monocyte-macrophage cells were grown in DMEM containing 10% FBS, 100 U/mL penicillin and 100 μg/mL streptomycin at 37 °C in a 5% CO_2 atmosphere [25]. Cells were seeded on 75 cm^2 flasks, sub-cultured using 10% EDTA.

2.6. Cell adhesion and proliferation

The adhesion and proliferation assays were performed as it was previously reported [26,27]. Briefly, cells were plated on the polymeric matrix in DMEM-10% FBS at a seeding density of 10^5 cell/mL and allowed to adhere for 1 h at 37 °C. For proliferation assay cells were incubated in the same conditions for 24 h. After each period of time, dishes were then washed with phosphate-buffered saline (PBS), fixed with 5% glutaraldehyde for 10 min and stained with crystal violet. The number of cells on the scaffolds was evaluated by microscopy counting several representative fields per well.

2.7. Evaluation of osteoblastic differentiation

Osteoblastic differentiation was evaluated by two markers: the quantitation of type I collagen production with a Sirius red-based colorimetric microssay and mineral nodule deposition [22].

Briefly, for type I collagen production, cells were fixed in Bouin's fluid for 1 h, washed with water and stained with Sirius red dye for 1 h. The stained material was dissolved in 0.1 N sodium hydroxide and the absorbance was read at 550 nm. For mineral nodule production cells were fixed with 4% p-formaldehyde and stained with alizarin S red. The nodules were de-stained in 0.1 N sodium hydroxide and the absorbance was read at 548 nm.

2.8. Interleukin-1b and tumor necrosis factor-α production

The cytotoxicity of the scaffold was evaluated measuring the production of the proinflammatory cytokine tumor necrosis factor alpha (TNF-α) and interleukin 1β (IL-1β). Briefly, macrophages RAW264.7 were plated on the scaffolds and the cytokine production was evaluated in the culture media after 7 days with ELISA (Mouse IL-1β ELISA Kit, OptEIA™ from BD Biosciences and Mouse TNF-α ELISA Kit, OptEIA™).

2.9. Degradation assay

To evaluate the possible degradation the membranes were weighted (W_o) and incubated with RAW264.7 macrophages in DMEM/10% FBS for 3 and 7 days. After that period cells were lysed with 0.1% Triton X-100, the scaffolds were washed several times with distilled water and dried until constant weight. After that the scaffolds were weighed again (W_t). Degradation was calculated as the weight loss of each scaffold during the culture period using the following expression:

$$\%\ \text{Degradation} = \frac{W_o - W_t}{W_o} 100. \quad (2)$$

In addition the average molecular weight of the material at the end of degradation assay (7 days) was analyzed by SEC.

2.10. Statistical analysis

Results are expressed as mean ± SEM and, unless indicated otherwise, were obtained from two separate experiments performed in triplicate. Differences between groups were assessed by one-way ANOVA with Dunnett multiple comparisons test and were performed using GraphPad InStat version 3.00 (GraphPad Software). A p value < 0.05 was considered significant for all statistical analyses.

3. Results and discussion

3.1. Preparation and characterization of the polymers

The copolymers obtained were identified by ^{1}H NMR (300 MHz, Chloroform-d_1, ppm) δ: 1.72 (h + l); 2.17 (g + i); 2.58 (j); 2.78 (m); 3.20 (k); 6.88 (c + f); 7.11 (b + e); and 7.21 (a + d). The copolymer compositions were estimated from the integral ratio of selected peaks of ^{1}H NMR, using the following formula: $F_{MOP} = (5I(Al) / (I(Ar) - 3)) / 3$, where I(Al) and I(Ar) are the intensity of the signals of aliphatic and aromatic hydrogen, respectively. The copolymer molecular weights were estimated from SEC measurements. The copolymers are named, St-co-MOP_1 and St-co-MOP_2. The chemical composition, weight-average molecular weight (M_w) and polydispersity index ($PI = M_w/M_n$) are: St-co-MOP_1, $F_{MOP} = 0.17$, $M_w = 82{,}400$ g/mol, IP = 1.99 and St-co-MOP_2, $F_{MOP} = 0.62$, $M_w = 33{,}200$ g/mol, IP = 2.07.

The chemical structure of the obtained copolymer is shown in Scheme 1. This scheme shows also, the tautomeric equilibrium present in the copolymer synthesized and the hydrogen assignation before indicated in the ^{1}H NMR spectrum.

3.2. Preparation and characterization of the scaffolds

St-co-MOP copolymers synthesized are functional materials characterized by the presence of tautomeric group, which can modulate the surface polarity depending of the environment as was demonstrated in a previous study [4]. This structural characteristic is significant considering the biomaterial–cell interaction, which is a key factor for the cell adhesion and proliferation process. On the other hand, some authors proposed that nanofibers, with high surface area to volume ratio and similar structural morphology to the fibrillar extracellular matrix, could be effective as tissue engineering scaffolds [28,29]. All these factors led us to study both the effect of St-co-MOP copolymer composition as well as the morphological characteristics of scaffolds on the biocompatibility of the samples.

The scaffolds were prepared by two different methods (solvent casting and nano-structuring) for comparison purposes. The surface of the scaffolds obtained by solvent casting was smooth, uniform and brittle as it was observed by SEM (Fig. 2A), while the membranes prepared using the self-ordered AAO templates showed a nanorod arrangement

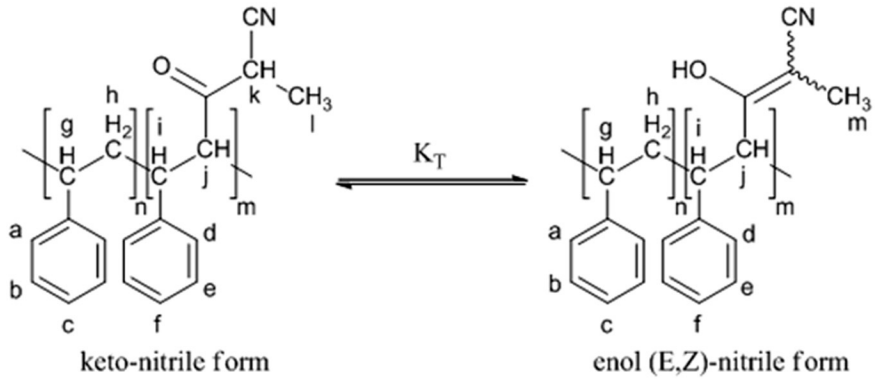

Scheme 1. Keto-enol equilibrium existing in St-co-MOP copolymer.

with a diameter of 270 nm and a length of 15 μm (Fig. 2B, arrow), so they could give differences in their biological response.

3.3. Cell morphology, adhesion and proliferation

Cells growing on the scaffold obtained by casting showed fibroblastoid morphology with good interactions between cells and with the substrate (Fig. 3A). Cells demonstrated cellular processes to interact with the flat surface (Fig. 3B, arrows). A similar morphology was observed in the osteoblasts growing on the nanostructured surfaces (Fig. 3C, arrows).

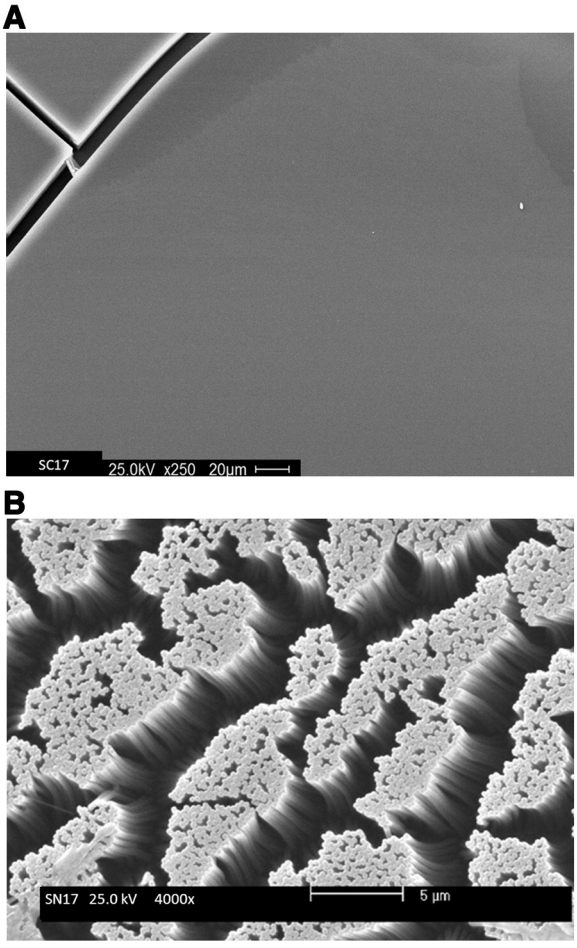

Fig. 2. Scanning electron microscopy (SEM) of the copolymers obtained by casting (A) or nanostructured in an AAO template (B).

However, cellular processes were shorter, with a ruffled like border and restricted to the nanorod exposed surface (Fig. 3D).

For biocompatibility assays osteoblastic cells were seeded on the scaffolds and allowed to adhere (1 h, adhesion assays) or to grow (24 h, proliferation assays). It is known that cell attachment is the first step toward the development of a tissue and the extent and the strength of cell adhesion to the matrix play a central role in the regulation of cell proliferation and differentiation. These processes depend strongly on the physical properties and chemical composition of the biomaterial surface [30,31]. In our experiments MC3T3E1 osteoblasts adhered better on the scaffolds obtained by casting than on the nanostructured ones or culture dishes (control) (Fig. 4). As expected, composition of the scaffold also influences cell adhesion: cells adhered better on scaffolds SC62 and SN62 in comparison to SC17 and SN17 (Fig. 4, $p < 0.01$).

In order to explain the adhesion results in relationship to the surface properties of the materials we evaluated the value of water contact angle (WCA) for the obtained scaffolds, which were present in Table 1. No significant differences were observed based on the different compositions but it was similar to the WCA value previously published for polystyrene (87°), a structurally-related polymer [32]. However, the nanostructured scaffolds showed a higher contact angle than casted scaffolds ($p < 0.01$). Similar behavior was previously described for other systems based on the same materials but with different surface topography [15]. In this case the measurement of an apparent contact angle with more hydrophobic character was attributed to air pockets trapped below the liquid, which could affect, at least initially the attachment of cells. In our scaffolds, the same effect could explain the differences observed in cell adhesion related to the different topographic characteristics, but it could not allow explain the differences related to the composition of the copolymer. In the last case, based on the chemical structure of our materials we estimate that in polar environment, such as culture media, the enol group will be predominant [4]. We assume that the presence of the enol functional moieties gives to the biomaterial the surface characteristics needed to support cell adhesion and proliferation, as it was reported before [33,34].

On the contrary, cells proliferating on the nanostructured surfaces grow better than those growing on the casted biomaterial (Fig. 5). Moreover osteoblastic proliferation on the nanorods was similar to the control. This result was not surprising since it has been previously demonstrated that cells with stronger interactions with the substrate proliferate in a less extent or even do not proliferate at all [35]. Cell adhesion must be a dynamic process where attached cells regulate proliferation signals. However, strong interaction with the biomaterial would conduce to a quiescent state where cells do not replicate but it can still differentiate [30].

3.4. Osteogenic differentiation

We next evaluated the osteogenic differentiation of MC3T3E1 cells on the tautomeric polymeric scaffolds. We found that type I collagen

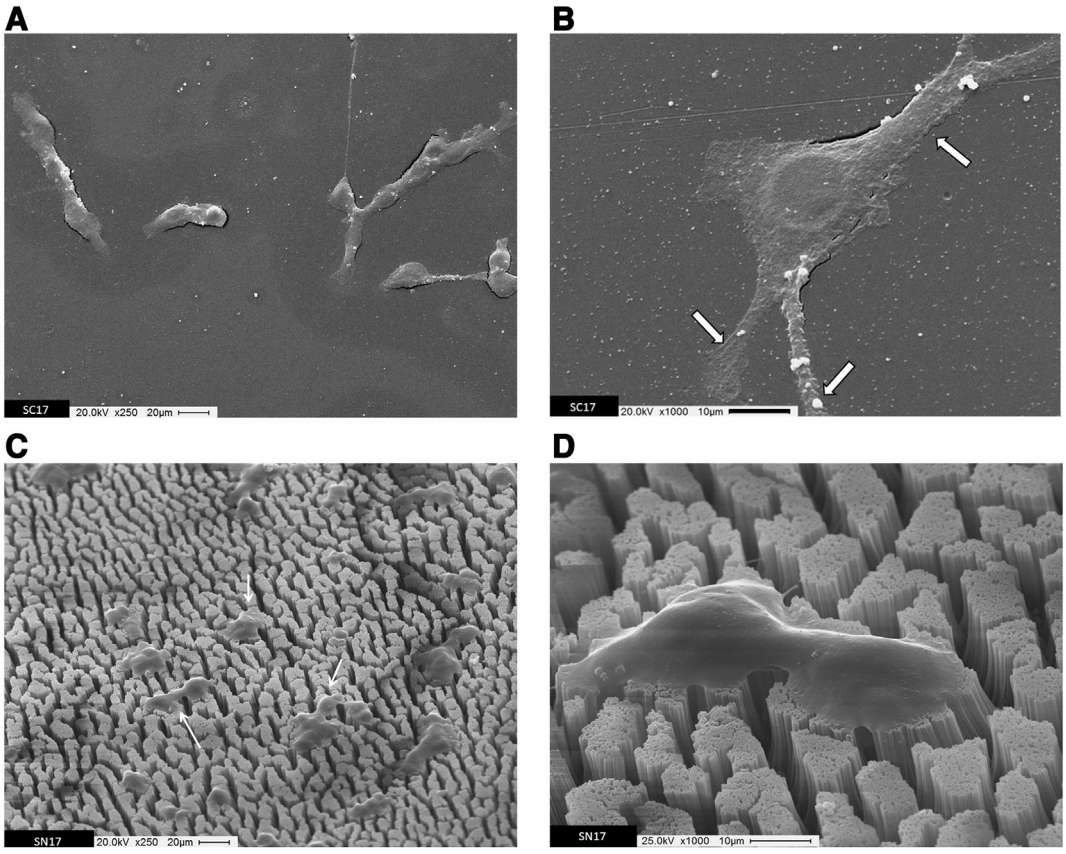

Fig. 3. Electronic microscopy (SEM) images of the osteoblastic cells growing on the scaffolds obtained by casting (A and B) or nanostructured (C and D). White arrows indicate the cellular processes of the osteoblasts interacting with the scaffolds. A and C 250× magnification; B and D 1000× magnification.

production was not influenced by the chemical composition of the scaffold or the presence of the nanofibers (Fig. 6A). Although, the presence of the nanorods showed a tendency to down regulate the secretion of type I collagen, this effect could be the consequence of the nanofibrillar organization of the biomaterial (Figs. 2B and 6A). Under this organization the osteoblastic cells interact with molecules similar in size to collagen therefore requiring less secretion of this protein to complete the extracellular matrix [36]. On the contrary, the mineralization of the matrix was significantly higher on the scaffolds with a lower MOP content but without significant differences on the surface morphology (Fig. 6B, $p < 0.001$). This behavior could be explained by the nature of cell interaction with the substrate e.g. a tight adhesion would favor cell differentiation [37], which was influenced by the poor development of the actin ring. We can speculate that in the biomaterials with lower MOP fraction the hydrophilicity of the biomaterial would not allow the correct assembly of the actin network, and as a result osteoblastic cells would not proliferate well but they are able to differentiate. On the other hand, the SN62 showed a tendency to mineralize the matrix in a greater extent than the same non-structured material (SC62, Fig. 6B). It has been previously demonstrated that the arrangement of the material at a nano size could improve osteogenesis compared to casted material [14,33,38]. In some cases it was observed that the nanostructuration of biomaterials for medical devices exhibited low reproducibility, this is not the case of our AAO templates, which presents the advantage of uniformity as well as a high reproducibility in the shape and size of the nanorods [33].

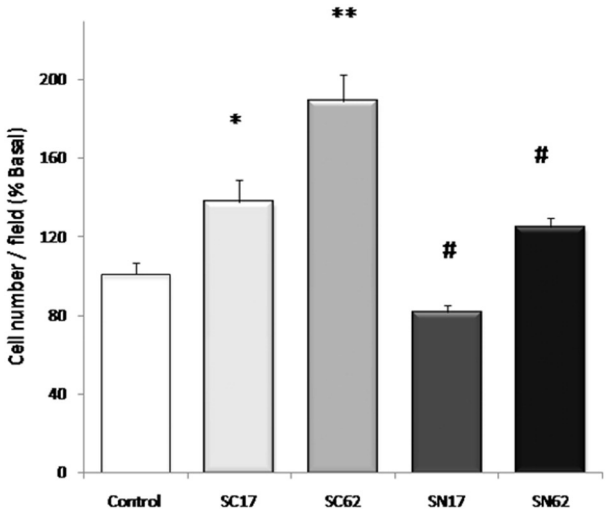

Fig. 4. Osteoblastic cell adhesion assay. Cells were allowed to adhere (1 h) and then evaluated by counting the number of cells by microscope field. n = 10, *p < 0.05 vs. control, **p < 0.01 vs. control; #p < 0.01 SC vs. SN.

3.5. Evaluation of scaffold cytotoxicity and degradation

It has been previously shown that macrophages are a very sensitive culture model to evaluate in vitro inflammatory responses to a material with potential applications in tissue engineering [11,39,40]. Thus, since

Table 1
Water contact angle of scaffolds obtained.

Scaffolds	WCA
SC17	90 ± 3**
SC62	90 ± 2*
SN17	102 ± 1
SN62	98 ± 1

** p < 0.01.
* p < 0.05 (SC vs SN).

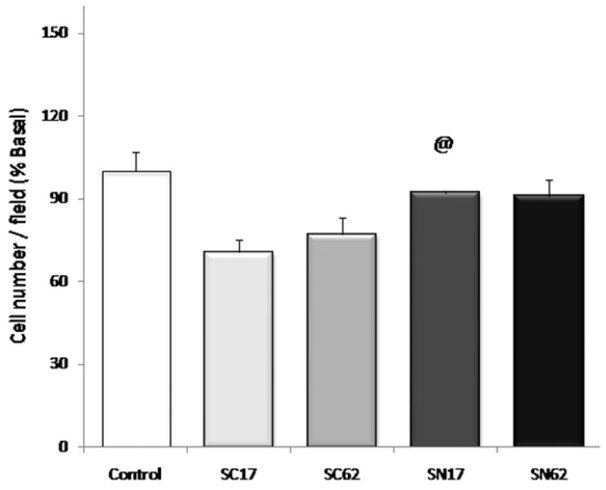

Fig. 5. Cell proliferation assay. After 24 h cells were fixed and evaluated by counting the number of cells by microscopic field. n = 10, @p < 0.05 SC vs. SN.

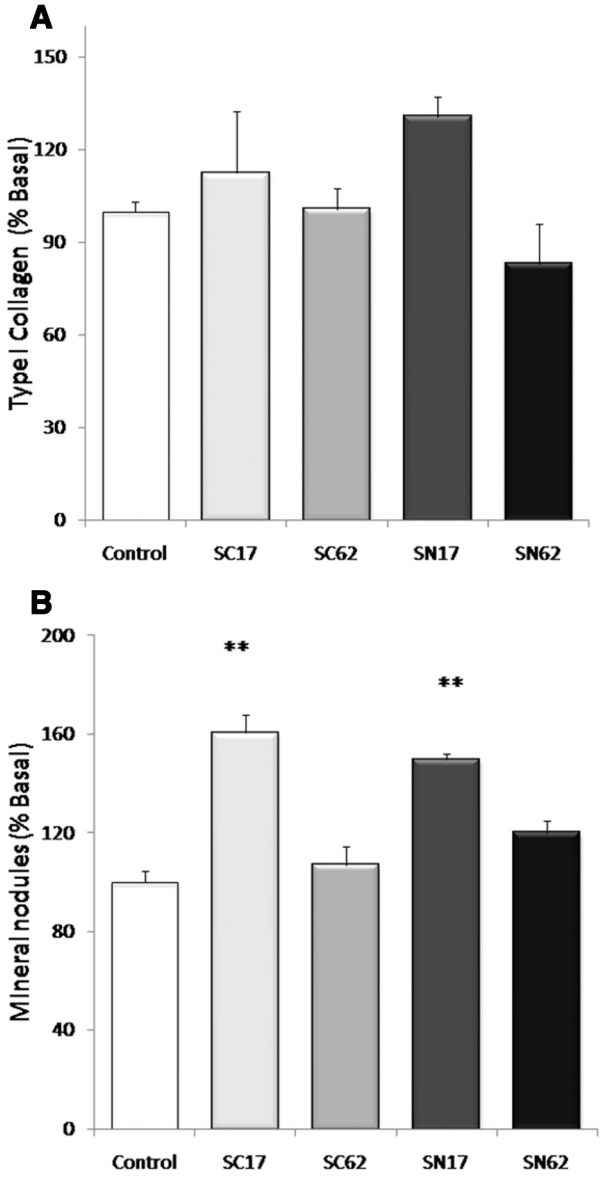

Fig. 6. Osteoblastic differentiation assay. (A) Type I collagen was evaluated by the colorimetric assay of Sirius red. (B) Mineral deposition was evaluated by the Alizarin S red colorimetric assay. **p < 0.01 vs. control.

the possible cytotoxic effect of our new biomaterial is a matter of great concern, we evaluated the production of two pro-inflammatory cytokines by RAW264.7 macrophages cultured on both scaffolds (SC and SN). We found that the cells growing on both kinds of surfaces produced very low levels of TNF-α and IL-1β and they were comparable to those produced by cells growing on control surfaces after 7 days of culture (Table 2). No differences were observed with composition or topography of the scaffolds, which suggest that these tautomeric copolymers are suitable as biomaterial.

Degradation time depends on the biomaterial properties itself (chemical structure and monomer composition) and on the availability of enzymes to degrade the synthetic matrix. Previously we demonstrated that synthetic polymer with a C–C main chain may be biodegradable by non-hydrolytic cellular mechanism, although at a slower rate than other biomaterials including heteroatom in their structure such as polyesters, and so on [22]. For degradation assays we cultured RAW264.7 macrophages on the scaffolds during 3 or 7 days, and after these periods of time the scaffolds were processed as indicated in the experimental section. In general, no significant change on the average molecular weight was observed at the maximum time assayed, as was determined by SEC (data not shown). The loss of weight showed that no significant degradation occurs after 3 days of culture. However, after 7 days of culture there was about 2.5% and 6% of loss of weight on the membranes obtained by casting and nanostructured respectively, although no differences were observed with the composition of the polymers (Fig. 7, $p < 0.01$). The apparent increase in the degradation of the nanostructured surfaces could be due to different effects, such as the greatest area of contact with the enzymes or the highest availability of water between the nanofibers which promote the erosion of materials. In fact, higher uptake of water of nanostructured than casted scaffolds was observed after 24 h (5.8% and 1.8% for SN and SC, respectively). A slow degradation rate is a desirable property of biomaterials used in bone tissue engineering because it should be consistent to the bone regeneration rate [41].

4. Conclusions

In conclusion we have developed and characterized a new kind of biomaterial with tautomeric properties. This material could be easily nanostructured in nanorods using a template mold of alumina. Under the experimental conditions evaluated we found significant differences in cell adhesion and proliferation processes in relation to surface morphology and copolymer composition, as well as a higher degradation of nanostructured scaffolds than casted scaffolds. This tautomeric copolymer showed a good biocompatibility and supports osteogenic differentiation with no induction of cytotoxicity and with degradation times that are compatible with bone regeneration times suggesting that it would be useful for bone tissue regeneration.

Acknowledgments

This research was partially supported by Grants from the Facultad de Ciencias Exactas, Universidad Nacional de La Plata (11/X644, UNLP), and Consejo Nacional de Investigación Científica y

Table 2
Cytotoxicity studies. TNF-α and IL-1β produced by RAW264.7 macrophages cultured on standard plastic tissue culture dishes (control), after 7 days of culture.

Sample	TNF-α (pg/mL)	IL-1β (pg/mL)
Control	9 ± 1	0.21 ± 0.01
SC17	8 ± 2	0.29 ± 0.05
SC62	6 ± 2	0.23 ± 0.02
SN17	9 ± 0.3	0.20 ± 0.03
SN62	7 ± 1	0.28 ± 0.06

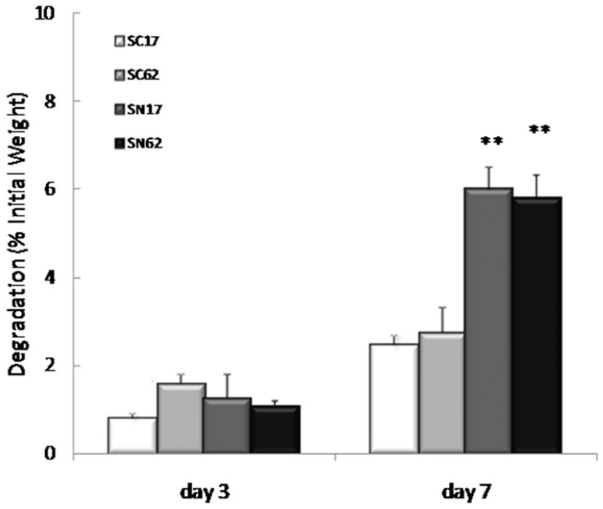

Fig. 7. In vitro degradation assay. Macrophage RAW264.7 cells were cultured on the scaffolds during different periods of time and then evaluated the loss of weight. $^{**}p < 0.01$ SN vs. SC.

Tecnológica (CONICET) (PIP-0035). MLL is Doctoral Fellow of UNLP. MSM is Investigador Adjunto of CONICET. MSC and PEA are a fulltime Researcher and Professor of UNLP. MINECO (PRIBRIBAR1011-1400 and MAT2011-24797) from Spain is also acknowledged.

References

[1] C. Deng, P.F. James, P.V. Wright, Poly(tetraethylene glycol malonate)-titanium oxide hybrid materials by sol–gel methods, J. Mater. Chem. 8 (1998) 153–159.
[2] P.C. Papaphilippou, A. Pourgouris, O. Marinica, A. Taculescu, G.I. Athanasopoulos, L. Vekas, T. Krasia-Christoforou, Fabrication and characterization of superparamagnetic and thermoresponsive hydrogels based on oleic-acid-coated Fe_3O_4 nanoparticles, hexa(ethylene glycol) methyl ether methacrylate and 2-(acetoacetoxy)ethyl methacrylate, J. Magn. Magn. Mater. 323 (2011) 557–563.
[3] N. Ohnishi, K. Aoshima, K. Kataoka, K. Ueno, Stimuli-responsive polymer utilizing keto-enol tautomerization and stimuli-responsive separating material and chemical-releasing capsule comprising the same, US Patent 7,732,550, (2010).
[4] J.M. Giussi, P.E. Allegretti, M.S. Cortizo, New copolymers of a tautomerizable β-ketonitrile monomer: synthesis, characterization and solution tautomerism, J. Polym. Sci. A Polym. Chem. 50 (2012) 4161–4169.
[5] J.M. Giussi, A. Ponzinibbio, M.S. Cortizo, P.E. Allegretti, 3-hydroxy-4-metil-4-pentenonitrile and 4-methyl-3-oxo-4-pentenonitrile: study of the tautomerics equilibria in gas phase and in solution, Spectrochim. Acta A Mol. Biomol. Spectrosc. 77 (2010) 367–373.
[6] R. Ravichandran, S. Sundarrajan, J.R. Venugopal, S. Mukherjee, S. Ramakrishna, Advances in polymeric systems for tissue engineering and biomedical applications, Macromol. Biosci. 12 (2012) 286–311.
[7] P.V. Kulkarni, C.A. Roney, P.P. Antich, F.J. Bonte, A.V. Raghu, T.M. Aminabhavi, Quinoline-n-butylcyanoacrylate-based nanoparticles for brain targeting for the diagnosis of Alzheimer's disease, Wiley Interdiscip. Rev. Nanomed. Nanobiotechnol. 2 (2010) 35–47.
[8] J.M. Giussi, I. Blaszczyk-Lezak, P.E. Allegretti, M.S. Cortizo, C. Mijangos, Tautomerizable styrenic copolymers confined in AAO templates, Polymer 54 (2013) 5050–5057.
[9] H. Cao, K. McHugh, S.Y. Chew, J.M. Anderson, The topographical effect of electrospun nanofibrous scaffolds on the in vivo and in vitro foreign body reaction, J. Biomed. Mater. Res. A 93 (2010) 1151–1159.
[10] F. Sun, H. Zhou, J. Lee, Various preparation methods of highly porous hydroxyapatite/polymer nanoscale biocomposites for bone regeneration, Acta Biomater. 7 (2011) 3813–3828.
[11] A.M. Cortizo, G. Ruderman, G. Correa, I.G. Mogilner, E.J. Tolosa, Effect of surface topography of collagen scaffolds on cytotoxicity and osteoblast differentiation, J. Biomater. Tissue Eng. 2 (2012) 125–132.
[12] B. Wang, Q. Cai, S. Zhang, X. Yang, X. Deng, The effect of poly (L-lactic acid) nanofiber orientation on osteogenic responses of human osteoblast-like MG63 cells, J. Mech. Behav. Biomed. Mater. 4 (2011) 600–609.
[13] V. Beachley, X. Wen, Polymer nanofibrous structures: fabrication, biofunctionalization, and cell interactions, Prog. Polym. Sci. 35 (2010) 868–892.
[14] J.M. Fernandez, M.S. Cortizo, A.M. Cortizo, G.A. Abraham, Osteoblast behavior on novel porous polymeric scaffolds, J. Biomater. Tissue Eng. 1 (2011) 86–92.
[15] M.P. Pavlov, J.F. Mano, N.M. Neves, R.L. Reis, Fibers and 3D mesh scaffolds from biodegradable starch-based blends: production and characterization, Macromol. Biosci. 4 (2004) 776–784.
[16] C.W. Lee, T.H. Wei, C.W. Chang, J.T. Chen, Effect of nonsolvent on the formation of polymer nanomaterials in the nanopores of anodic aluminum oxide templates, Macromol. Rapid Commun. 33 (2012) 1381–1387.
[17] J. Martin, M.J. Maiz, J. Sacristan, C. Mijangos, Tailored polymer-based nanorods and nanotubes by "template synthesis": from preparation to applications, Polymer 53 (2012) 1149–1166.
[18] J. Martin, C. Mijangos, Tailored polymer-based nanofibers and nanotubes by means of different infiltration methods into alumina nanopores, Langmuir 25 (2009) 1181–1187.
[19] S. Grimm, J. Martin, G. Rodriguez, M. Fernandez-Gutierrez, K. Mathwig, R.B. Wehrspohn, U. Gosele, J. San Roman, C. Mijangos, M. Steinhart, Cellular interactions of biodegradable nanorod arrays prepared by nondestructive extraction from nanoporous alumina, J. Mater. Chem. 20 (2010) 3171–3177.
[20] M.S. Cortizo, H.A. Andreetta, R.V. Figini, Molecular characterization of poly(diisopropylfumarate) by the absolute calibration method in molecular exclusion chromatography (GPC), J. High Resolut. Chromatogr. Chromatogr. Commun. 12 (1989) 372–374.
[21] J.M. Fernandez, M.S. Molinuevo, A.M. Cortizo, A.D. McCarthy, M.S. Cortizo, Characterization of poly-ε-caprolactone/polyfumarate blends as scaffolds for bone tissue engineering, J. Biomater. Sci. Polym. Ed. 21 (2010) 1297–1312.
[22] M.S. Cortizo, M.S. Molinuevo, A.M. Cortizo, Biocompatibility and biodegradation of polyesters and polyfumarates based-scaffold for bone tissue engineering, J. Tissue Eng. Regen. Med. 2 (2008) 33–42.
[23] M.S. Cortizo, J.L. Alessandrini, S.B. Etcheverry, M.S. Cortizo, A vanadium/aspirin complex controlled release using a poly(b-propiolactone) film. Effects on osteosarcoma cells, J. Biomater. Sci. Polym. Ed. 12 (2001) 945–959.
[24] L.D. Quarles, D.A. Yohay, L.W. Lever, R. Caton, R.J. Wenstrup, Distinct proliferative and differentiated stages of murine MC3T3-E1 cells in culture: an in vitro model of osteoblast development, J. Bone Miner. Res. 7 (1992) 683–692.
[25] M.S. Molinuevo, S.B. Etcheverry, A.M. Cortizo, Macrophage activation by a vanadyl–aspirin complex is dependent on L-type calcium channel and the generation of nitric oxide, Toxicology 210 (2005) 205–212.
[26] A.M. Cortizo, C. Sedlinsky, A.D. McCarthy, A. Blanco, L. Schurman, Osteogenic actions of the anti-diabetic drug metformin on osteoblasts in culture, Eur. J. Pharmacol. 536 (2006) 38–46.
[27] A.D. McCarthy, T. Uemura, S.B. Etcheverry, A.M. Cortizo, Advanced glycation endproducts interfere with integrin-mediated osteoblastic attachment to a type-I collagen matrix, Int. J. Biochem. Cell Biol. 36 (2004) 840–848.
[28] J. Chen, B. Zhou, Q. Li, J. Ouyang, J. Kong, W. Zhong, M.M. Xing, PLLA-PEG-TCH-labeled bioactive molecule nanofibers for tissue engineering, Int. J. Nanomedicine 6 (2011) 2533–2542.
[29] S. Kidoaki, I.K. Kwon, T. Matsuda, Mesoscopic spatial designs of nano- and microfiber meshes for tissue-engineering matrix and scaffold based on newly devised multilayering and mixing electrospinning techniques, Biomaterials 26 (2005) 37–46.
[30] L. Bacakova, E. Filova, M. Parizek, T. Ruml, V. Svorcik, Modulation of cell adhesion, proliferation and differentiation on materials designed for body implants, Biotechnol. Adv. 29 (2011) 739–767.
[31] B.K. Mann, J.L. West, Cell adhesion peptides alter smooth muscle cell adhesion, proliferation, migration, and matrix protein synthesis on modified surfaces and in polymer scaffolds, J. Biomed. Mater. Res. 60 (2002) 86–93.
[32] Y. Li, J.Q. Pham, K.P. Johnston, P.F. Green, Contact angle of water on polystyrene thin films: effects of CO_2 environment and film thickness, Langmuir 23 (2007) 9785–9793.
[33] H.N. Kim, A. Jiao, N.S. Hwang, M.S. Kim, D.H. Kang, D.H. Kim, K.Y. Suh, Nanotopography-guided tissue engineering and regenerative medicine, Adv. Drug Deliv. Rev. 65 (2013) 536–558.
[34] X. Liu, J.Y. Lim, H.J. Donahue, R. Dhurjati, A.M. Mastro, E.A. Vogler, Influence of substratum surface chemistry/energy and topography on the human fetal osteoblastic cell line hFOB 1.19: phenotypic and genotypic responses observed in vitro, Biomaterials 28 (2007) 4535–4550.
[35] R. Yamaguchi, Y. Mazaki, K. Hirota, S. Hashimoto, H. Sabe, Mitosis specific serine phosphorylation and down regulation of one of the focal adhesion protein, paxillin, Oncogene 15 (1997) 1753–1761.
[36] I.O. Smith, X.H. Liu, L.A. Smith, P.X. Ma, Nanostructured polymer scaffolds for tissue engineering and regenerative medicine, Wiley Interdiscip. Rev. Nanomed. Nanobiotechnol. 1 (2009) 226–236.
[37] M. Vandrovcova, T. Douglas, D. Hauk, B. Grossner-Schreiber, J. Wiltfang, L. Bacakova, P.H. Warnke, Influence of collagen and chondroitin sulfate (CS) coatings on poly-(lactide-co-glycolide) (PLGA) on MG 63 osteoblast-like cells, Physiol. Res. 60 (2011) 797–813.
[38] Z.G. Zhang, Z.H. Li, X.Z. Mao, W.C. Wang, Advances in bone repair with nanobiomaterials: mini-review, Cytotechnology 63 (2011) 437–443.
[39] M. Bixby, L. Spieler, T. Menini, A. Gugliucci, *Ilex paraguariensis* extracts are potent inhibitors of nitrosative stress: a comparative study with green tea and wines using a protein nitration model and mammalian cell cytotoxicity, Life Sci. 77 (2005) 345–358.
[40] L.C. Denlinger, P.L. Fisette, K.A. Garis, G. Kwon, A. Vazquez-Torres, A.D. Simon, B. Nguyen, R.A. Proctor, P.J. Bertics, J.A. Corbett, Cell biology and metabolism, J. Biol. Chem. 271 (1996) 337–342.
[41] Y.H. An, K.L. Martin, Handbook of Histology Methods for Bone and Cartilage, in: Y.H. An, K.L. Martin (Eds.), Humana Press, Totowa, New Jersey, USA, 2003.